



HAL
open science

The most recent burst of star formation in the massive elliptical galaxy NGC 1052

J. A. Fernandez-Ontiveros, C. Lopez-Sanjuan, M. Montes, M. A. Prieto, J. A. Acosta-Pulido

► **To cite this version:**

J. A. Fernandez-Ontiveros, C. Lopez-Sanjuan, M. Montes, M. A. Prieto, J. A. Acosta-Pulido. The most recent burst of star formation in the massive elliptical galaxy NGC 1052. *Monthly Notices of the Royal Astronomical Society*, 2011, 411 (1), pp.L21–L25. 10.1111/j.1745-3933.2010.00985.x . hal-01438055

HAL Id: hal-01438055

<https://hal.science/hal-01438055>

Submitted on 30 Nov 2021

HAL is a multi-disciplinary open access archive for the deposit and dissemination of scientific research documents, whether they are published or not. The documents may come from teaching and research institutions in France or abroad, or from public or private research centers.

L'archive ouverte pluridisciplinaire **HAL**, est destinée au dépôt et à la diffusion de documents scientifiques de niveau recherche, publiés ou non, émanant des établissements d'enseignement et de recherche français ou étrangers, des laboratoires publics ou privés.



Distributed under a Creative Commons Attribution 4.0 International License

The most recent burst of star formation in the massive elliptical galaxy NGC 1052*

J. A. Fernández-Ontiveros,^{1,2†} C. López-Sanjuan,³ M. Montes,^{1,2} M. A. Prieto^{1,2}
and J. A. Acosta-Pulido^{1,2}

¹*Instituto de Astrofísica de Canarias (IAC), Vía Láctea s/n, La Laguna E-38200, Spain*

²*Departamento de Astrofísica, Facultad de Física, Universidad de La Laguna, Astrofísico Fco. Sánchez s/n, La Laguna E-38207, Spain*

³*Laboratoire d'Astrophysique de Marseille, Pôle de l'Etoile Site de Château-Gombert 38, rue Frédéric Joliot-Curie, F-13388 Marseille, France*

Accepted 2010 November 9. Received 2010 October 8; in original form 2010 April 7

ABSTRACT

High spatial resolution near-infrared (NIR) images of the central 24×24 arcsec² ($\sim 2 \times 2$ kpc²) of the elliptical galaxy NGC 1052 reveal a total of 25 compact sources randomly distributed in the region. 15 of them exhibit H α luminosities an order of magnitude above the estimate for an evolved population of extreme horizontal branch stars. Their H α equivalent widths and optical-to-NIR spectral energy distributions are consistent with them being young stellar clusters aged < 7 Myr. We consider this to be the first direct observation of spatially resolved star-forming regions in the central kiloparsecs of an elliptical galaxy. The sizes of these regions are $\lesssim 11$ pc and their median reddening is $E(B - V) \sim 1$ mag. According to previous works, NGC 1052 may have experienced a merger event about 1 Gyr ago. On the assumption that these clusters are spread with a similar density over the whole galaxy, the fraction of galaxy mass (5×10^{-5}) and rate of star formation ($0.01 M_{\odot} \text{ yr}^{-1}$) involved suggest the merger event as the possible cause for the star formation we see today.

Key words: techniques: high angular resolution – galaxies: individual: NGC 1052 – galaxies: interactions – galaxies: nuclei – galaxies: star clusters: general.

1 INTRODUCTION

About ~ 30 per cent of the local early-type galaxies present signs of recent star formation (RSF) in the last Gyr (Kaviraj et al. 2007). This result arises from the study of the integrated ultraviolet–optical (UV–optical) colours of a large sample of early-type galaxies. A sizeable fraction of objects are revealed by their blue colours, $\text{NUV} - r < 5.5$ mag, where NUV stands for near-UV, despite the fact that their optical colours place them in the optical ‘red sequence’ ($u - r > 2.2$ mag, Strateva et al. 2001). Given these blue $\text{NUV} - r$ colours, a merger is likely the origin of the induced RSF (Kaviraj et al. 2009; Kaviraj 2010; López-Sanjuan et al. 2010).

In that scenario, one would expect the formation of new young cluster populations in an elliptical galaxy, which presents blue UV–optical colours and a past merger event (Kaviraj 2010). However, most of the examples reported up to date exhibit intermediate-age clusters between $\gtrsim 200$ Myr and a few Gyr (e.g. NGC 1316, 1380, 1700, 3610 and 5128, Carlson et al. 1999; Goudfrooij et al. 2001;

Williams et al. 2010). In those cases, most of the age estimates are based on the comparison of cluster colours with stellar population models and thus are strongly dependent on the metallicity, extinction and initial mass function assumed in these models. Therefore, a scrutinized study of nearby ellipticals with blue UV–optical colours is particularly interesting to reveal the young cluster population at the earliest stage of their evolution, that is, $\lesssim 10$ Myr. It is in this context that this Letter is addressed. It presents the first detection of individually resolved young stellar clusters (YSCs), $\lesssim 7$ Myr old, in a nearby elliptical galaxy NGC 1052. To single out this population, high spatial resolution imaging from UV to optical and infrared (IR) is used. A complete spectral energy distribution (SED) is built for each of the clusters, and their nature, ages and dust estimates have been addressed on the basis of their H α emission.

NGC 1052 is one of the nearest elliptical galaxies (E4, 18 Mpc, $1 \text{ arcsec} \approx 87$ pc, Jensen et al. 2003) with a stellar mass of $M_{\star} \approx 10^{11} M_{\odot}$ (derived from 2MASS¹ photometry, assuming $M_{\star}/L_K = 1.32 M_{\odot}/L_{\odot}$, Cole et al. 2001) and a low-level activity LINER nucleus (Heckman 1980). It presents two radio lobes (Cooper, Lister & Kochanzyk 2007, fig. 1) and a collimated ionized gas structure in H α +[N II] (Pogge et al. 2000), both extended in the east–west

*Based on European Southern Observatory (ESO) Very Large Telescope (VLT) program 076.B-0493 and *Hubble Space Telescope* (HST) program IDs 3639, 6286, 7403 and 7886.

†E-mail: jaf@iac.es

¹Two-Micron All-Sky Survey, see <http://www.ipac.caltech.edu/2mass/>

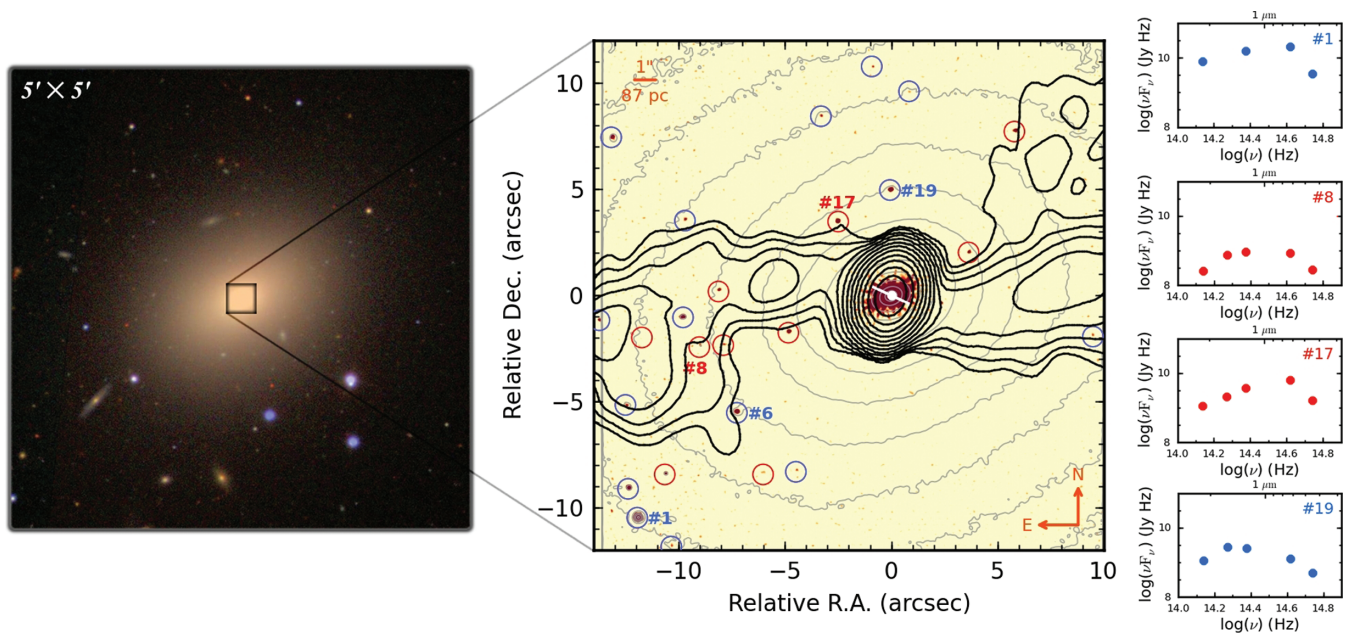


Figure 1. Left-hand panel: SDSS g - (blue), r - (green) and i -band (red) colour composite image for NGC 1052. VLT/NaCo 24×24 -arcsec² FOV is marked by a black square. Middle panel: unsharp-masked VLT/NaCo K_s -band image, logarithmic contours for the natural K_s -band image (grey colour) and VLA contours at 1.4 GHz (black, beam $\sim 2 \times 1.5$ arcsec², Cooper et al. 2007). Knots with $\text{EWH}\alpha \geq 50 \text{ \AA}$ are given in blue and in red are given those with $\text{EWH}\alpha < 50 \text{ \AA}$. The central white barred-dot marks the position of the nucleus and the direction of the parsec-scale twin jet. Right-hand panel: SEDs for two ‘blue’ (#1 and #19) and two ‘red’ knots (#8 and #17).

direction, and a parsec-scale twin jet ($\text{PA} \sim 60^\circ$) with an emission gap between the brightest part located north-east (NE) and the counter jet located in the south-west (SW) direction (Kadler et al. 2004). The radio lobes are also spatially coincident with the X-ray-emission region reported by Kadler et al. (2004). The distribution of the H I gas, with two tidal tails extended from NE to SW and also an infalling component, is interpreted as evidence of a merger event about 1 Gyr ago (van Gorkom et al. 1986, 1989). This scenario is further supported by the different rotation axes found for the gas and the stars (Plana & Boulesteix 1996) and by the presence of dust lanes along the N–S direction near the galaxy centre (Forbes, Sparks & Macchetto 1990). Furthermore, NGC 1052 shows typical integrated colours of a ‘rejuvenated’ early-type galaxy (following Kaviraj et al. 2007), having $\text{NUV} - r = 4.9$ mag, while the $u - r = 2.8$ mag colour places this galaxy in the optical red sequence (NUV from Rampazzo et al. 2007; u and r bands from the SDSS²).

2 OBSERVATIONS

The brightness of the LINER nucleus permitted us to perform high spatial resolution observations using the VLT and the Nasmyth Adaptive Optics System (NAOS) plus the near-infrared imager and spectrograph (CONICA). The VLT/NaCo data set consists of near-IR (NIR) J -, K_s - and L' -band observations for the central 24×24 arcsec² of NGC 1052 ($\sim 2 \times 2$ kpc², Fig. 1), taken on 2005 December 3. The total exposure times are 900 s (J), 400 s (K_s) and 5.25 s (L'), and the achieved full width at half-maximum (FWHM) resolutions – measured in the most compact objects in these images – are $\lesssim 0.26$, $\lesssim 0.12$ and $\lesssim 0.12$ arcsec, respectively. Data reduction of the NaCo data set was performed using the

ECLIPSE package, provided by the ESO, and includes sky subtraction, registration and combination of frames to obtain a final image per filter. The photometric calibration was based on standard stars taken along with the science frames. The relative photometric error is ~ 8 , ~ 11 and ~ 11 per cent in the J , K_s and L' bands, respectively. The VLT/NaCo data set was complemented with the following *HST* imaging: WFPC/F555W (Wide Field Planetary Camera/V-band, $\lambda 0.55 \mu\text{m}$ $\Delta\lambda 0.05 \mu\text{m}$), WFPC2/F658N (including $\text{H}\alpha + [\text{N II}]$, $\lambda 0.659 \mu\text{m}$ $\Delta\lambda 0.003 \mu\text{m}$), STIS/F28X50LP (Space Telescope Imaging Spectrograph, $\lambda 0.72 \mu\text{m}$ $\Delta\lambda 0.11 \mu\text{m}$) and NICMOS/F160W (Near-Infrared Camera and Multi-Object Spectrometer/ H -band, $\lambda 1.61 \mu\text{m}$ $\Delta\lambda 0.12 \mu\text{m}$). The reduced images were retrieved directly from the scientific archive and the photometric calibration was performed by using the PHOTFLAMB keyword value in the image header as a conversion factor.

Image alignment of the whole set is based on the identification of two compact sources (knots) seen in all filters, but in the L' band. We avoided using the nucleus since dust obscuration may distort its position in the optical. For the L' band, we assumed its position to match that in the K_s band. We further used a 1.4-GHz image with a beam resolution of $\sim 2 \times 1.5$ arcsec² from the Very large Array (VLA) (Cooper et al. 2007). The signal-to-noise ratio achieved in the NaCo J and K_s bands permitted us to distinguish a number of point-like sources in the field of view (FOV). In order to enhance the image contrast, different techniques were applied, the best results being obtained by the unsharp-masking method (Sofue 1993). A median circular filter with radius 0.12 arcsec was used to smooth the images, which were then subtracted from the original ones. The result for the K_s band is shown in the background of Fig. 1. The DAOPHOT finding algorithm (Stetson 1987) recovered, on the J and K_s unsharp-masked images, a total of 25 point-like sources over a 3σ threshold in the central 24×24 arcsec² (circles in Fig. 1). None of these knots are detected in the UV images from the *HST*/ACS

² Sloan Digital Sky Survey, see <http://www.sdss.org/>.

(Advance Camera for Surveys), acquired with the $F250W$ and $F330W$ filters, and also taken from the scientific archive. The wider FOV of the STIS image ($\sim 28 \times 51$ arcsec 2) shows nearly 70 knots, which seem more dispersed with increasing radius. Counterparts in other bands ($F555W$, J , K_s , none detected in the L' band) exist only for the 25 knots in the common FOV. In the H band, two of these knots are outside the NICMOS FOV. The photometry was extracted from a circular aperture ($r_a = \text{FWHM}$ in each filter) centred on a common position for all images. The background emission was then subtracted as the mode value for an annular concentric region [$r_s \sim (0.4\text{--}0.6)$ arcsec]. Some of these regions stand out in the narrow-band $F658N$ image, centred on $H\alpha + [\text{N II}]$. To estimate the flux in this blend, the continuum contribution was inferred by linear interpolation between the $F555W$ and J broad-band filters. The possible uncertainties derived in the continuum estimation will be discussed later. Finally, the $H\alpha$ flux was then corrected by the $[\text{N II}]$ contribution by assuming that to be 40 per cent of the total (Baldwin, Phillips & Terlevich 1981).

3 RESULTS

Most of the 25 knots are unresolved or barely resolved with sizes of about 0.12 arcsec ($\lesssim 10.5$ pc), that is, the spatial resolution in the VLT/NaCo K_s -band image. They show a median brightness of $m_K = 20.9$ mag, which corresponds to an absolute magnitude of $M_K = -10.4$ mag, too bright for being individual red supergiant stars (Tabur, Kiss & Bedding 2009). The knots are distributed in the $-12 \leq M_K \leq -9$ mag range, except knot #1, which is by far the brightest with $M_{K\#1} = -13.6$ mag. In the optical, they are characterized by a median $m_V = 24.3$ mag and $m_I = 22.1$ mag, corresponding to $M_V = -7.0$ mag and $M_I = -9.2$ mag. Most of the 25 knots are strong emitters in $H\alpha$. Moreover, the $H\alpha$ equivalent width ($\text{EWH}\alpha$) distribution shows $\gtrsim 50$ Å for most of them; we therefore adopted this value as a threshold to separate $H\alpha$ -emitting knots from those without $H\alpha$ emission. Assuming these to be star clusters, their ages were derived from their $\text{EWH}\alpha$. STARBURST99 models (Leitherer et al. 1999) were used, assuming an instantaneous burst model with the highest available metallicity, $Z = 0.04$. This follows the results by Pierce et al. (2005) who found higher than solar metallicity abundances ($Z > 0.08$) in the central ~ 10 arcsec (~ 1 kpc) region of NGC 1052 from the analysis of spectral indices measured at various radii in an optical long-slit spectrum. Note that these are stellar metallicities and not nebular ones. A lower limit for the metallicity will be considered below.

A total of 15 knots were found with $\text{EWH}\alpha \geq 50$ Å (blue circles in Fig. 1), which yields ages of $\lesssim 6.8$ Myr. Their median $\text{EWH}\alpha$ value is 116 Å (6.2 Myr), with half of them located in the 105–175 Å range (5.4–6.5 Myr), that is, the first and third quartiles, respectively. Lower $\text{EWH}\alpha$ for the remaining knots may be due to the clusters being older or due to a higher extinction, which will affect the $H\alpha$ continuum interpolation. In the conservative side, choosing larger photometric aperture in the $F555W$ and J bands – the ones used to define the $H\alpha$ continuum flux – decreases the number of knots over the 50 Å limit to eight, instead of 15. The net effect of considering lower metallicities, for example, $Z = 0.001$, would translate in older ages for a given $\text{EWH}\alpha$, but values over the 50 Å threshold still limit the age to ≤ 12.2 Myr. The number of ‘young’ regions just increases to 16 by assuming the $[\text{N II}]$ contribution to be 20 per cent instead of 40 in the $H\alpha + [\text{N II}]$ blend.

The $H\alpha$ luminosity ($L_{H\alpha}$) for the 15 knots with $\text{EWH}\alpha \geq 50$ Å spans the $(1\text{--}33) \times 10^{36}$ erg s $^{-1}$ range. Notwithstanding, ionizing photons may be produced by an old stellar population due to the

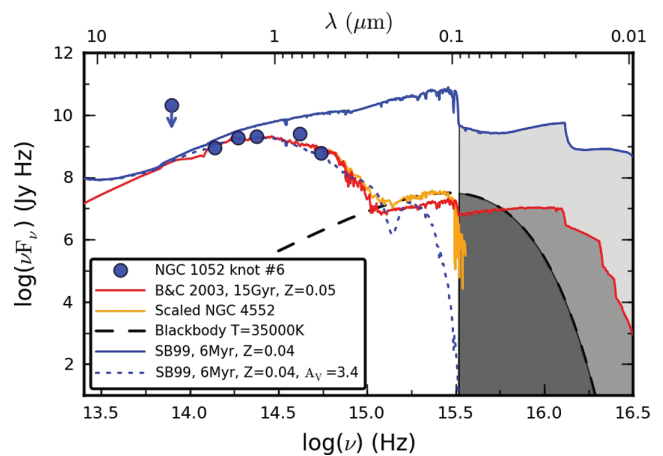


Figure 2. Knot #6 SED (blue circles) compared with a 15-Gyr, $Z = 0.05$ template (Bruzual & Charlot 2003, red line), a composite spectrum of NGC 4552 (Yi, Demarque & Oemler 1998, yellow line) plus a blackbody spectrum ($T = 35\,000$ K, black-dashed line), and a 6-Myr, $Z = 0.04$ template from STARBURST99 (Leitherer et al. 1999, blue-solid line), also shown with an obscuration of $A_V = 3.4$ mag (blue-dotted line). Shaded areas correspond to photons with $\lambda \leq 910$ Å.

‘UV-upturn’ (see O’Connell 1999, and references therein). This additional contribution in the UV range originates in some low-mass, helium-burning stars in the extreme horizontal branch (EHB) and subsequent phases of evolution. In this scenario, the compact knots in NGC 1052 could be either old globular clusters (GCs) with an EHB component or YSCs probably linked with the merger event occurred in the recent history of this galaxy. A detailed analysis was then performed for knot #6 (Fig. 1), which is representative of the 15 knots’ sample in terms of the brightness and SED’s shape. From its $H\alpha$ luminosity (5.2×10^{36} erg s $^{-1}$), we derived an ionizing photon rate of $\sim 3.8 \times 10^{48}$ photon s $^{-1}$ (following Osterbrock 1989). This estimate is compared in the following sections with predictions of a SED from an old and a young stellar population.

3.1 Old globular clusters?

Fig. 2 shows the SED of knot #6, which is derived from broad-band photometry (blue dots), including the upper limit in the L' band. First, we show the SED of a 15-Gyr-old, $Z = 0.05$ population from Bruzual & Charlot (2003, red line in Fig. 2) scaled to the NIR SED of knot #6 (the NIR SED comprises three points: $HST/F160W$, NaCo J and K_s bands). We choose scaling to the NIR to minimize dust extinction effects. The rate of ionizing photons produced by this population – mainly by blue horizontal branch stars – is then determined by integrating the template below the Lyman limit (shaded area below the red line). This results in 1.2×10^{47} photon s $^{-1}$, that is, more than an order of magnitude lower than the value measured for knot #6; thus, the $H\alpha$ emission cannot be explained by this 15-Gyr-old population.

However, the EHB component is not included in the 15-Gyr-old template. EHB stars present small envelopes around the helium core, showing a hot thermal spectrum with $T \gtrsim 20\,000$ K. The integrated energy distribution of such an old population ($\gtrsim 10$ Gyr) increases shortwards of ~ 2000 Å and is thus capable of emitting far-UV photons (Greggio & Renzini 1990). To estimate the possible contribution of these stars, we consider the spectrum of the UV-strong elliptical galaxy NGC 4552, which is expected to have an important contribution from EHB stars. For consistency, this

spectrum was scaled to the 15-Gyr-old template used before in the optical region (yellow line in Fig 2). Shortwards of 900 Å, the NGC 4552 spectrum was extended with a $T = 35\,000$ K blackbody that was scaled to NGC 4552 in the UV part (black-dashed line in Fig. 2). In this case, the integrated number of ionizing photons is 1.8×10^{47} photon s^{-1} , still an order of magnitude below the measured value. It should be noted that the measured $H\alpha$ emission in the knots, and thus the ionizing photon rate, may still be a lower limit due to the possible contribution of $H\alpha$ in absorption. This is expected from intermediate-age A-star population in the clusters.

3.2 Young stellar clusters?

We now consider a young 6-Myr-old, $Z = 0.04$ star cluster model from STARBURST99 (blue-solid line in Fig. 2, Leitherer et al. 1999). The model choice is based on the EWH α of knot #6. Scaling it to the NIR SED region of this knot, the resulting photon rate is 2.5×10^{49} photon s^{-1} . This is more than an order of magnitude larger than the measured value. Moreover, the model largely overestimates the emission in the optical range (see Fig. 2). As dust is expected in the environment of young clusters, different extinction values were applied to this model till both, the observed SED luminosity and the $H\alpha$ luminosity, were matched. We started with an initial value of $A_V = 2.5$ mag – inferred from the $H\alpha$ ratio between the model and observation – and applied it consecutively to the SED. The process of fitting both the $H\alpha$ emission and the SED shape was done in an iterative manner (using the extinction curve by Cardelli, Clayton & Mathis 1989). The best match was found for a model with $A_V = 3.4$ mag (blue-dotted line in Fig. 2), which reproduces the shape of the measured SED. The intrinsic photon rate inferred from the model is 4.9×10^{49} photon s^{-1} , $L_{H\alpha} \sim 6.6 \times 10^{37}$ erg s^{-1} and mass $1.3 \times 10^4 M_\odot$ (from K_s -band luminosity, assuming an age– M/L_K dependence from Leitherer et al. 1999). Note that, as we are assuming a foreground dust screen, these values may be lower limits.

3.3 Colours

All the 25 knots look different in brightness and colours with respect to those of the GCs studied in the outer 2–20 kpc of this galaxy by Pierce et al. (2005). The latter present a median $m_V \sim 22.0$ mag with $V - I \sim 0.9$ mag, in contrast with the $V - I = 2.4$ mag³ shown by the former (Fig. 3). Note that the *HST*/F28X50LP filter is even bluer than the *I* band. The differences suggest that both populations are intrinsically distinct. This filter also includes the $H\alpha + [N II]$ blend (~ 0.660 μm at $z = 0.005$) very close to the transmission peak,⁴ but this contribution to the broad-band magnitude (~ 0.3 dex for knot #6) is not enough to explain the large difference in the $V - I$ colour. Only knot #1 has an $m_V = 21.9$ mag, compatible with that of the GCs, but its $V - I$ colour is much redder (2.6 mag).

This discrepancy between the two populations cannot be ascribed to the colour bimodality reported by Forbes et al. (2001), since all the GCs in this study lie in the range $1.2 < V - I < 1.7$ mag. On the other hand, an obscuration of $A_V = 3.4$ mag may explain why the knots in the central region look much redder than those of the GCs. Similar extinction values and colours to those shown by the knots have been reported for YSCs in the starburst galaxies NGC

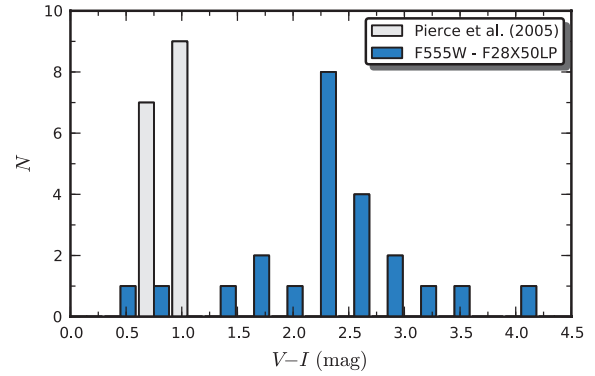


Figure 3. In grey, $V - I$ colours for the GCs in the outer 2–20 kpc of NGC 1052 (Pierce et al. 2005). In blue, the $F555W - F28X50LP$ colour for the 25 knots identified in the central $\sim 2 \times 2$ kpc².

5253 (Vanzi & Sauvage 2004) and NGC 253 (Fernández-Ontiveros, Prieto & Acosta-Pulido 2009).

4 DISCUSSION

RSF is found in the centre (2×2 kpc²) of NGC 1052 in the form of young (~ 6 Myr) and compact (~ 14 pc) stellar clusters with masses of $\sim 10^4 M_\odot$. The age estimation does not depend strongly on the stellar population model assumed. The total star formation rate (SFR) in the centre, derived from the $H\alpha$ luminosity of the 25 knots, is $SFR \sim 7 \times 10^{-4} M_\odot \text{ yr}^{-1}$ (following Kennicutt 1998). Assuming that these clusters are spread with a similar density over the whole galaxy results in an upper limit for the SFR of $\sim 0.01 M_\odot \text{ yr}^{-1}$. The resulting specific SFR places the galaxy in the ‘red and death’ sequence ($SFR/M_* \lesssim 10^{-12} \text{ yr}^{-1}$, Fontana et al. 2009). Even if we consider the extrapolation for the whole galaxy, the total mass forming these clusters would be less than 5×10^{-3} per cent of the galaxy stellar mass. This suggests that the current RSF is not dominant in the present evolution of NGC 1052.

Several observational signatures indicate that NGC 1052 experienced a merger in the last 1 Gyr (cf. Introduction). The origin of the knots may be associated with left over activity from that event. Hydrodynamical N -body merger simulations (mass ratio 1:6–1:10) by Peirani et al. (2010) suggest that star formation occurs in several bursts after the merger event rather than being a continuous process (see also Kaviraj et al. 2009). This is in agreement with the observations: we find two very young clusters (EWH $\alpha \sim 230$ Å; ~ 5.1 Myr), four young ones ($140 \leq \text{EWH}\alpha < 200$ Å; 5.2–5.6 Myr), seven slightly older ones ($90 \leq \text{EWH}\alpha < 140$ Å; 5.6–6.6 Myr) and 12 with $\text{EWH}\alpha < 90$ Å (> 6.6 Myr). This means that *we are probably looking at either the final stage or a minimum in the star formation activity in the centre induced by a merger event*. In their simulations, Kaviraj et al. (2009) explore extinction values in the $E(B - V) = 0 - 0.5$ mag range, showing that observations favour those models with higher extinction [$E(B - V) \gtrsim 0.3$ mag]. For comparison, the colour excess of knot #6 suggests higher values, that is, $E(B - V) \sim 1.1$ mag ($A_V \sim 3.4$ mag).

Regarding their spatial distribution, the knots with $\text{EWH}\alpha \geq 50$ Å are located randomly and do not seem to follow any special pattern except for a weak preference for the NW–SE direction. Moreover, we do not find any clear connection with either the kpc-scale radio lobes at 1.4 GHz (Fig. 1) or the extended emission in X-rays detected by *Chandra* (Kadler et al. 2004). This indicates that the recent star

³ Strictly speaking, the $F555W - F28X50LP$ colour.

⁴ <http://www.stsci.edu/hst/stis/design/filters/>

formation episode in the centre is not, at least directly, driven by nuclear activity.

The lack of high spatial resolution CO maps does not allow us to connect the knots with density enhancements in the cold material, but the dust lanes in the N–S direction seen in the STIS image are not apparently related with the knots. However, this scattered star formation is in line with the ‘widespread’ star formation mode found by Shapiro et al. (2010) for early-type galaxies with multiple and mismatched kinematic components. This is the case of NGC 1052, which shows two counter-rotating gaseous components decoupled from the stellar kinematics (Plana & Boulesteix 1996). Furthermore, Shapiro et al. (2010) find that those objects with very low SFRs ($\lesssim 0.06 M_{\odot} \text{ yr}^{-1}$) exhibit a more centralized star formation activity, which is also favoured by recent simulations (Peirani et al. 2010). This might explain why Forbes et al. (2001) and Pierce et al. (2005) did not find young clusters in their study, as they covered the outskirts of NGC 1052 (2–20 kpc). Nevertheless, an $H\alpha$ image with a wider FOV is needed to check the young cluster distribution on scales larger than the inner few kpc.

Since we determine the age of the knots on the basis of $H\alpha$ emission, we are only sensitive to very recent star-formation episodes ($\lesssim 10 \text{ Myr}$) and cannot provide a reliable age for those knots with $\text{EWH}\alpha < 50 \text{ \AA}$ (10 out of the 25). However, these show very similar properties (i.e. sizes, magnitudes, colours) to those with $\text{EWH}\alpha > 50 \text{ \AA}$, are also randomly distributed and their SEDs are qualitatively similar (see Fig. 1). Results from stellar population models on the integrated spectrum of the central $\sim 1 \text{ kpc}$ indicate luminosity-weighted ages of $\sim 2 \text{ Gyr}$ (Pierce et al. 2005). However, the contribution of the 25 knots reported in this work is not sufficient to ‘rejuvenate’ the integrated emission of the central region. In line with the scenario proposed by Shapiro et al. (2010), a middle-age population ($10 \text{ Myr} < t < 2 \text{ Gyr}$) is still needed, which would be probably related with a more intense star formation episode in the past. A spatially resolved spectroscopic study of the central kpc region would be enlightening.

5 FINAL REMARKS

We propose that the knots found in the centre of NGC 1052 are YSCs formed in a very RSF episode, probably related with the merger event that occurred $\sim 1 \text{ Gyr}$ ago (van Gorkom et al. 1986). This is the first detection of resolved YSCs in the centre of an elliptical galaxy. Their presence has three major implications: (i) we are looking at the final stage of the RSF occurring in the central parsecs of NGC 1052; (ii) the RSF takes place in the form of compact and YSCs similar to those found in starburst galaxies; and (iii) the reddening predicted by YSC templates [$E(B - V) \sim 1.1 \text{ mag}$] should be explored in future simulations of these systems, which used to assume a lower value as an upper limit.

The case of NGC 1052 is probably one of the best examples for the study of the recent evolution of nearby early-type galaxies via merging with gas-rich satellites. However, high spatial resolution observations in dynamically younger remnants, for which we expect

a larger number of YSCs, are desired to understand in detail the role of mergers in the present evolution of elliptical galaxies.

ACKNOWLEDGMENTS

The authors acknowledge A. Marín-Franch for his useful hints on globular cluster physics and M. Orienti for reviewing the radio data. This work is partially funded by the Spanish MEC project AYA2007-60235.

REFERENCES

- Baldwin J. A., Phillips M. M., Terlevich R., 1981, *PASP*, 93, 5
 Bruzual G., Charlot S., 2003, *MNRAS*, 344, 1000
 Cardelli J. A., Clayton G. C., Mathis J. S., 1989, *ApJ*, 345, 245
 Carlson M. N. et al., 1999, *AJ*, 117, 1700
 Cole S. et al., 2001, *MNRAS*, 326, 255
 Cooper N. J., Lister M. L., Kochanzyk M. D., 2007, *ApJS*, 171, 376
 Fernández-Ontiveros J. A., Prieto M. A., Acosta-Pulido J. A., 2009, *MNRAS*, 392, L16
 Fontana A. et al., 2009, *A&A*, 501, 15
 Forbes D. A., Georgakakis A. E., Brodie J. P., 2001, *MNRAS*, 325, 1431
 Forbes D. A., Sparks W. B., Macchetto F. D., 1990, *NASA Conference Publication*, 3098, 431
 Goudfrooij P. et al., 2001, *MNRAS*, 322, 643
 Greggio L., Renzini A., 1990, *ApJ*, 364, 35
 Heckman T. M., 1980, *A&A*, 87, 152
 Jensen J. B. et al., 2003, *ApJ*, 583, 712
 Kadler M. et al., 2004, *A&A*, 420, 467
 Kaviraj S., 2010, *MNRAS*, 408, 170
 Kaviraj S. et al., 2007, *ApJS*, 173, 619
 Kaviraj S. et al., 2009, *MNRAS*, 394, 1713
 Kennicutt R. C., Jr, 1998, *ARA&A*, 36, 189
 Leitherer C. et al., 1999, *ApJS*, 123, 3
 López-Sanjuan C. et al., 2010, preprint (arXiv:1009.5921)
 O’Connell R. W., 1999, *ARA&A*, 37, 603
 Osterbrock D. E., 1989, *Astrophysics of Gaseous Nebulae and Active Galactic Nuclei*. Univ. Science Books, Mill Valley, CA
 Peirani S. et al., 2010, *MNRAS*, 405, 2327
 Pierce M. et al., 2005, *MNRAS*, 358, 419
 Plana H., Boulesteix J., 1996, *A&A*, 307, 391
 Pogge R. W., Maoz D., Ho L. C., Eracleous M., 2000, *ApJ*, 532, 323
 Rampazzo R. et al., 2007, *MNRAS*, 381, 245
 Shapiro K. L. et al., 2010, *MNRAS*, 402, 2140
 Sofue Y., 1993, *PASP*, 105, 308
 Stetson P. B., 1987, *PASP*, 99, 191
 Strateva I. et al., 2001, *AJ*, 122, 1861
 Tabur V., Kiss L. L., Bedding T. R., 2009, *ApJ*, 703, L72
 van Gorkom J. H. et al., 1986, *AJ*, 91, 791
 van Gorkom J. H. et al., 1989, *AJ*, 97, 708
 Vanzì L., Sauvage M., 2004, *A&A*, 415, 509
 Williams B. F. et al., 2010, *ApJ*, 716, 71
 Yi S., Demarque P., Oemler A. J., 1998, *ApJ*, 492, 480

This paper has been typeset from a \LaTeX file prepared by the author.